

Synthesis of Liquid Crystal Molecules Based on Bis(biphenyl)diacetylene and Their Liquid Crystallinity

Makoto Uchimura, Sungmin Kang, Rohei Ishige, Junji Watanabe,* and Gen-ichi Konishi*

Department of Organic and Polymeric Materials, Tokyo Institute of Technology,
O-okayama, Meguro-ku, Tokyo 152-8552

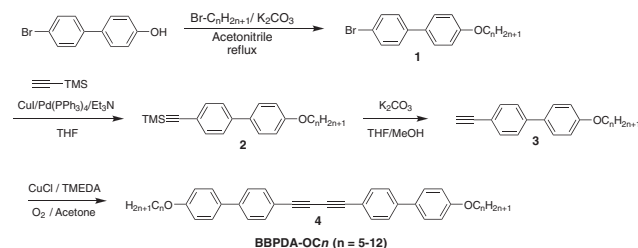
(Received March 3, 2010; CL-100200; E-mail: jwatanab@polymer.titech.ac.jp, konishi.g.aa@m.titech.ac.jp)

We synthesized novel liquid crystalline molecules that contain a bis(biphenyl)diacetylene mesogen and confirmed their structures by ^1H NMR, ^{13}C NMR, and FT-IR spectroscopy and mass spectrometry. These compounds formed thermotropic liquid crystals in a wide temperature region that was well characterized by optical microscopic and X-ray measurements.

During the course of studies to explore new mesogenic groups, we synthesized liquid crystalline (LC) materials based on a bis(biphenyl)diacetylene [BBPDA, bis(biphenyl)butadiyne] moiety. This moiety consists of only hydrocarbons. In other words, it, irrespective of its remarkably long axial ratio, does not possess dipolar groups such as esters, azomethine, and amides. Thus, the interaction between molecules in a liquid crystalline field may be characteristic and distinct from those in other polar LC molecule systems. Further, this moiety should afford high birefringence to the liquid crystal because of its anisotropic polarization.^{1–4} To realize these points, in this study, we synthesized bis(biphenyl)diacetylenes containing alkoxy tail groups (BBPDA-OC n , n : carbon number in alkoxy tail), and analyzed their liquid crystalline behavior.

BBPDA-OC n s were synthesized according to Scheme 1. First, 4-alkoxy-4'-bromobiphenyls with $n = 5–12$ were synthesized by the Williamson ether reaction. Second, 4-alkoxy-4'-ethynylbiphenyls were prepared by the palladium-catalyzed Sonogashira coupling, followed by base-induced hydrolysis. Finally, BBPDA-OC n s were obtained by the Glaser coupling. The structures of the obtained compounds were confirmed by ^1H NMR, ^{13}C NMR, and FT-IR spectroscopy and mass spectrometry (see Supporting Information).¹¹ The ^{13}C NMR spectrum of BBPDA-OC8 is shown in Figure 1. Characteristic peaks can be observed at 82.0 and 74.6 ppm; these are assigned to the diacetylene unit. Further, we synthesized asymmetric BBPDA-OC5–11 by using compounds 3 with different carbon numbers of 5 and 11. The product was separated by HPLC and purified by recrystallization to obtain pure BBPDA-OC5–11.

The thermal behaviors of BBPDA-OC n ($n = 5–12$) and BBPDA-OC5–11 were investigated by differential scanning



Scheme 1. Synthesis of BBPDA-OC n derivatives.

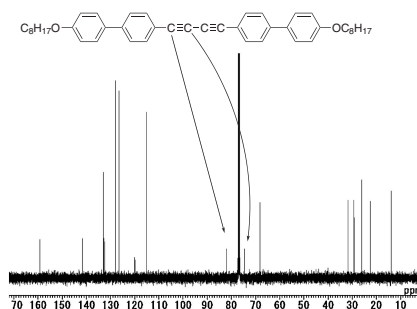


Figure 1. ^{13}C NMR spectrum of BBPDA-OC8 (100 MHz, CDCl_3).

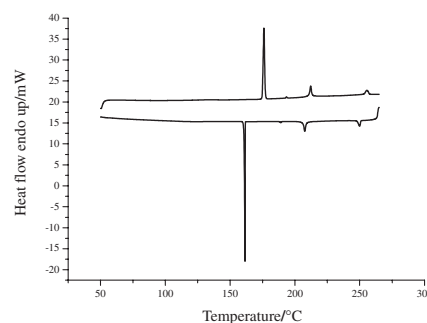


Figure 2. Typical DSC thermogram of BBPDA-OC8.

calorimetry (DSC). The representative DSC curves of BBPDA-OC8 are shown in Figure 2 (refer to Figures S6–S12 for other samples). As observed from the figure, several clear transitions can be detected. The phase transition temperatures and enthalpy changes were measured during the cooling scan, and these are listed in Table 1. In Figure 3, the transition temperatures are plotted against the carbon number of the alkoxy tail. Four types of mesophases—nematic, Sm C, Sm I, and Sm J—can be well distinguished in a wide temperature region, although a nematic-to-isotropic transition cannot be detected in all these compounds because of the extremely high transition temperature. Thus, a high isotropization temperature and wide mesophase temperature region are characteristic of this molecular system. The former is caused by the high axial ratio of mesogen, and the latter may be attributable to the nonpolar nature of mesogen.

The shortest homolog, BBPDA-OC5, exhibits only a nematic (N) LC. BBPDA-OC6 forms N, Sm C, and Sm I phases. In BBPDA-OC n s with $n = 7, 8, \text{ and } 9$, the Sm I phase transforms to the Sm J phase, and is followed by relatively low enthalpy changes of around 1.0 kJg^{-1} . This enthalpy change decreases with an increase in n ; in longer homologs with $n = 10$,

Table 1. Phase transition temperature ($^{\circ}\text{C}$) and enthalpies (ΔH , kJ mol^{-1}) (in italics) for the BBPDA-OC n series and BBPDA-OC5–11 obtained from cooling DSC thermograms at a rate of $10^{\circ}\text{C min}^{-1}$

n	Phase behavior and transition temperature (enthalpy)
5	N 211.2 (44.61) Cr
6	N 213.9 (1.74) Sm C 201.3 (7.43) Sm I 195.0 (28.7) Cr
7	N 236.0 (1.62) Sm C 207.7 (6.47) Sm I 197.6 (0.76) Sm J 179.0 (32.2) Cr
8	N 250.0 (2.27) Sm C 210.2 (5.67) Sm I 191.8 (0.60) Sm J 164.1 (23.5) Cr
9	N 257.7 (3.19) Sm C 210.3 (5.32) Sm I 182.4 (0.22) Sm J 154.2 (21.1) Cr
10	Sm C 209.4 (5.93) Sm I (or Sm J) 148.0 (19.8) Cr1 127.6 (7.47) Cr ₂
11	Sm C 207.5 (4.07) Sm I (or Sm J) 143.3 (16.5) Cr1 111.7 (5.35) Cr ₂
12	Sm C 205.7 (4.34) Sm I (or Sm J) 138.4 (18.1) Cr1 116.3 (14.4) Cr ₂
5–11	N 239.8 (2.78) Sm C 199.9 (12.7) Sm I 171.5 (0.42) Sm J 137.2 (48.3) Cr

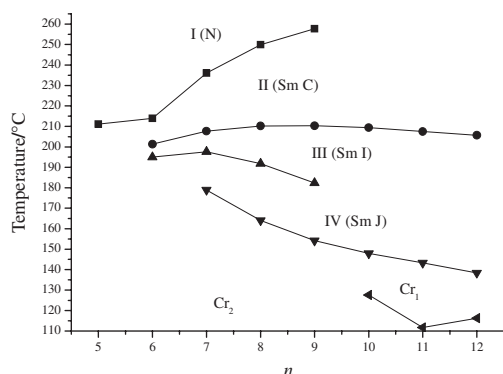


Figure 3. Phase behavior of BBPDA-OC n s.

11, and 12, no distinct transition can be detected in the DSC thermogram although some change can be detected by polarized optical microscopy. Asymmetric BBPDA-OC5–11 exhibited four phase transitions. Its transition behavior is similar to that of BBPDA-OC8, which has a similar molecular length, however the mesophase temperature region is wider than those of symmetric compounds.

In order to reveal the detailed mesophase structure, all the compounds were analyzed by wide angle X-ray diffractometry (WAXD). Typical WAXD patterns obtained for the mesophases of BBPDA-OC7 are shown in Figure 4. Here, the sample was aligned homeotropically on a glass plate that is surface-treated by organo-silane coupling agents,⁵ and then the X-ray beam is irradiated parallel to the glass surface.

The WAXD pattern shown in Figure 4a is that for the highest-temperature nematic phase. It exhibits an inner streak with a spacing of 34.4 \AA and an outer broad reflection with a spacing of 4.5 \AA , characteristic of a nematic phase. Because the streaks in the inner zone are clearly split, a cybotactic nematic

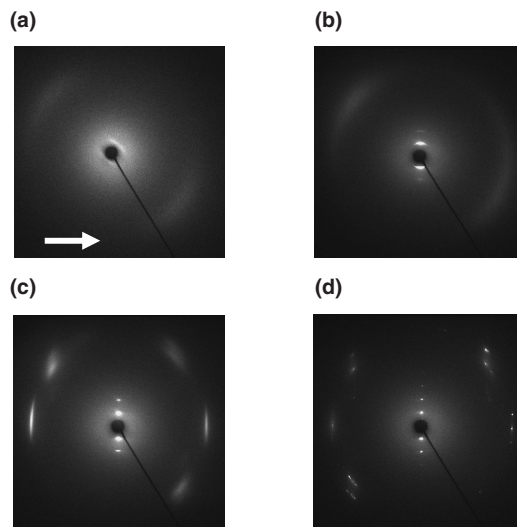


Figure 4. WAXD patterns of BBPDA-OC7. (a) Nematic (245°C), (b) Sm C (220°C), (c) Sm X1 (200°C), and (d) Sm X2 (186°C). Here, the X-ray patterns were obtained for a homeotropically oriented sample on a glass plate with the beam parallel to the glass surface. The arrow indicates the glass surface direction.

phase is likely; the nematic LC is formed by cybotactic groups composed of about 10^2 molecules with the molecular center in each groups arranged in layers.⁶

Here, it is noteworthy that the director orients in a tilted direction to the glass surface. This situation can be easily understood from a comparison with the X-ray pattern of nematic LC aligned by the magnetic field shown in Figure S1, where the director corresponds to the magnetic field direction. One of the maximum positions in an inner streak is on a meridional direction and an outer broad reflection is observed 50° apart from the equatorial line. Such an unusual orientation is attributable to the cybotactic association of molecules in such a manner that the pseudo layer formed by the cybotactic groups lies parallel to the glass surface.⁶ On reflecting this orientation, the Sm C phase appearing on cooling exhibits a more concrete orientation with layer reflection on a meridional direction and a broad outer reflection 40° apart from the equatorial direction (Figure 4b). In the Sm I phase, the layer reflection on the meridian becomes narrower, indicating that the orientation of the layer is improved. Simultaneously the outer reflections become sharper and appear at six positions (Figure 4c). Three sets of these reflections have similar spacings of 4.35 \AA . Among them, two sets of reflections are observed at the same angular position as that observed in the Sm C phase, and another set is observed along the equator. Such a pattern can be explained by the improved packing order within a layer; the molecules within a layer are packed with a more definite hexagonal lattice and the molecular tilting is directed toward the apex of the hexagonal lattice, as illustrated in Figure 5. This is characteristic of the Sm I phase.^{7,8} The X-ray pattern of the Sm J phase is essentially similar to that of the Sm I phase, except that it is more improved so that all of the reflections appear as very sharp spots (Figure 4d). The additional sharp spots observed immediately above the six (100) reflections are assigned to (101). This

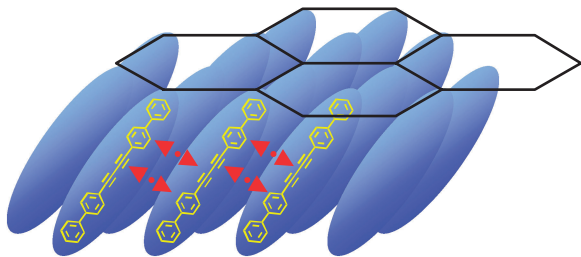


Figure 5. Structure of Sm I phase where the molecules tilt to the layer and are locally packed into a hexagonal lattice.

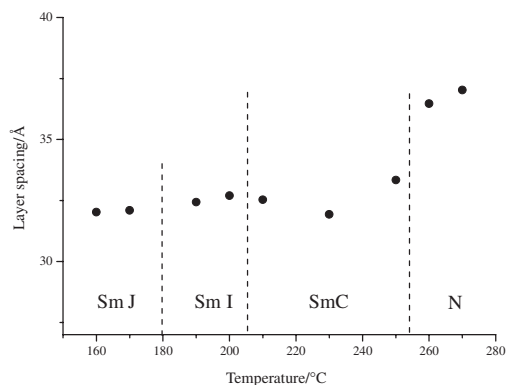


Figure 6. Temperature dependence of layer spacing of BBPDA-OC9 through the transitions from nematic to Sm J phases.

improved diffraction profile indicates the long-range periodic ordering within the layers and between the layers. These are characteristics of the Sm (or crystal) J phase.⁹

It should be noted that the spacing of the layer reflection is maintained through the phase transition from the nematic to the Sm J phase. This can be seen in Figure 6, which shows the temperature dependence of the layer spacing. The collected spacings for all compounds are compared with the molecular lengths in Table 2. The tilt angles elucidated from a comparison of the two parameters are also listed in Table 2. They do not depend on the carbon number of the alkoxy tail, and are found to range from 41 to 44°. These values correspond to those elucidated (36 to 40°) from the X-ray patterns shown in Figures 4b–4d.

The large tilt angle and its independency of the temperature and alkoxy tail length are probably caused by the special interaction between mesogenic moieties. Figure 5 shows BBPDA-OC n molecules associated into a layer with a tilt angle of 40°. It is obvious that in this association, the phenyl groups of one molecule are near the acetylene groups in the neighboring

Table 2. Carbon number dependence of tilt angle

n	Layer spacing/Å		Tilt angle /°
	Experimental	Calculated	
6	28.6	37.9	41.1
7	30.1	39.9	41.1
8	30.8	42.8	44.0
9	32.3	44.8	43.9
10	34.6	47.7	43.5
11	36.7	49.7	42.4
12	38.9	52.6	42.3

molecule. Such an interesting association is observed in the crystal structure of bis(biphenyl)diacetylene reported by Constable et al.,¹⁰ suggesting strong interaction between biphenyl and diacetylene moieties.

In summary, we synthesized bis(biphenyl)diacetylenes containing an alkoxy group (BBPDA-OC n s) and analyzed their liquid crystalline behaviors. The long nonpolar mesogen provides a wide mesogenic temperature region, including the nematic, Sm C, Sm I, and Sm J phases. Irrespective of this polymorphism, the tilting association of molecules giving a large tilt angle of 40° is invariably observed; this is due to the specific interaction between phenyl and acetylene groups.

References and Notes

- 1 H. Takatsu, K. Takeuchi, Y. Tanaka, M. Sasaki, *Mol. Cryst. Liq. Cryst.* **1986**, *141*, 279.
- 2 S.-T. Wu, H. B. Meng, L. R. Dalton, *J. Appl. Phys.* **1991**, *70*, 3013.
- 3 S.-T. Wu, J. D. Margerum, H. B. Meng, L. R. Dalton, C.-S. Hsu, S.-H. Lung, *Appl. Phys. Lett.* **1992**, *61*, 630.
- 4 Y. Kitani, C. Kitamura, A. Yoneda, N. Kawatsuki, *Mol. Cryst. Liq. Cryst.* **2005**, *443*, 181.
- 5 J. Thisayukta, H. Takezoe, J. Watanabe, *Jpn. J. Appl. Phys.* **2001**, *40*, 3277.
- 6 A. de Vries, *Mol. Cryst. Liq. Cryst.* **1970**, *10*, 219.
- 7 A. J. Leadbetter, J. P. Gaughan, B. Kelly, G. W. Gray, J. Goodby, *J. Phys. (Paris)* **1979**, *40*, 178.
- 8 P. A. C. Gane, A. J. Leadbetter, P. G. Wrighton, *Mol. Cryst. Liq. Cryst.* **1981**, *66*, 247.
- 9 J. Goodby, in *Handbook of Liquid Crystals*, ed. by D. Demus, J. Goodby, G. W. Gray, H.-W. Spiess, Wiley-VCH, Weinheim, **1998**, Vol. 2A, p. 17.
- 10 E. C. Constable, D. Gusmeroli, C. E. Housecroft, M. Neuburger, S. Schaffner, *Acta Crystallogr., Sect. C* **2006**, *62*, o505.
- 11 Supporting Information is available electronically on the CSJ-Journal Web site, <http://www.csj.jp/journals/chem-lett/index.html>.